13th World Conference on Earthquake Engineering
Vancouver, B.C., Canada
August 1-6, 2004
Paper No. 2935

BASE-ISOLATION TECHNIQUES FOR THE SEISMIC PROTECTION OF RC FRAMED STRUCTURES SUBJECTED TO NEAR-FAULT GROUND MOTIONS

Fabio MAZZA[1] and Alfonso VULCANO[2]

SUMMARY

The main objective of this work is to compare different base-isolation techniques, in order to evaluate their effects on the structural response and applicability limits under near-fault earthquakes. In particular, high-damping-laminated-rubber bearings are considered, in case acting in parallel with supplemental viscous dampers, or acting either in parallel or in series with steel-PTFE sliding bearings. A numerical investigation is carried out assuming as reference test structure a base-isolated five-storey reinforced concrete (r.c.) framed building designed according to Eurocode 8 (EC8) provisions. A bilinear model idealizes the behaviour of the r.c. frame members, while the response of the elastomeric bearings is simulated by using a viscoelastic linear model; a viscous-linear law and a rigid-plastic one are assumed to simulate the seismic behaviour of a supplemental damper and a sliding bearing, respectively. The seismic analysis of the test structures, subjected to strong ground motions recorded near faults, is carried out by using a step-by-step procedure.

INTRODUCTION

The base-isolation techniques prove to be very effective for the seismic protection of new framed buildings as well as for the seismic retrofitting of existing ones. Design guidelines have been developed in many countries with a high seismic hazard (e.g., United States, Japan, New Zealand) and, lately, suitable code provisions have been drafted also in Europe (Eurocode 8 [1]). However, under near-fault ground motions, even base-isolated structures designed according to recent seismic codes can undergo unforeseen structural damages.

The near-fault ground motions are characterized by long duration pulses, with displacements so large that an oversizing of the isolation system could be required (Kelly [2], Mazza et al. [3]). Moreover, the frequency content of the motion transmitted by the isolators to the superstructure can become critical when the pulse intensity is such that the superstructure undergoes plastic deformations (Vestroni et al.

[1] Research Assistant, Dipartimento di Strutture, Università della Calabria, Arcavacata di Rende (Cosenza), Italy. Email: fmazza@unical.it
[2] Professor, Dipartimento di Strutture, Università della Calabria, Arcavacata di Rende (Cosenza), Italy. Email: vulcano@unical.it

[4]). In addition, it is possible an amplification of the structural response due to the long duration of the pulse. Actually, EC8 recommends that site-specific spectra including near source effects should be taken into account for buildings of importance class I (e.g., hospitals and nuclear plants) located at a distance less than 15 km from the nearest potentially active fault with a magnitude $M_s \geq 6.5$.

To overcome the above mentioned problems many authors (e.g., Mazza et al. [3], Jangid et al. [5], Makris et al. [6]) proposed solutions based on different kinds of isolators and dampers. The main objective of the present work is to compare some of the base-isolation techniques more frequently adopted in literature with reference to framed buildings subjected to far-fault earthquakes (e.g., Jangid et al. [5], Dolce et al. [7]), in order to evaluate their effects on the structural response and applicability limits under near-fault earthquakes. To this aim, a numerical investigation is carried out with reference to typical base-isolated five-storey r.c. framed buildings designed according to EC8. The dynamic response of the test structures isolated at the base by elastomeric bearings, in case acting in combination with supplemental dampers or sliding bearings, is studied considering strong ground motions recorded near faults in Turkey (1999, 2003) and Greece (1986, 1999).

BASE ISOLATION SYSTEMS

The base isolation systems are usually realized by elastomeric and sliding bearings, if necessary combined with supplemental dampers. The main typologies of isolation systems proposed in literature to provide an acceptable seismic performance of framed structures are outlined below (for a more detailed discussion see, e.g., Naeim et al. [8], Skinner et al. [9]).

The elastomeric-type bearings, e.g. those of a high-damping type (i.e., like the “High-Damping-Laminated-Rubber Bearing”, HDLRB) or fiber-reinforced (Kelly [10]), filter the ground motion so that the effects on the response of the superstructure are reduced. A lead core may be inserted in the laminated bearing (like the “Lead-Rubber Bearing”, LRB) to increase both the initial stiffness, so limiting the base displacement under seismic actions of moderate intensity and wind actions, and the hysteretic energy dissipation. On the other hand, for the frictional-type bearings (e.g., sliding bearings with a steel-PTFE interface or rolling bearings like the “Friction-Pendulum”, FP) the maximum acceleration transmitted to the superstructure is limited through a frictional force proportional to the supported weight. However, the structure behaves like a fixed-base structure during the stick-phases. Moreover, residual base displacements are expected for the frictional bearings, because no restoring force is provided.

The horizontal force-displacement (F-u) law of an elastomeric bearing can be idealized using the viscoelastic linear model in figure 1a (e.g., in the case of a HDLRB) or the bilinear model in figure 1b (e.g., in the case of a LRB), but the above law has to be properly modified as shown in figure 1c, to take into account the hardening effects at large strains levels; while the rigid-plastic model shown in figure 1d can be adopted to represent a frictional bearing. Moreover, different responses (e.g., see the elasto-viscoplastic model in figure 1e and the trilinear model in figure 1f) are expected when elastomeric and frictional bearings or isolation and supplemental damping systems at the base are combined (e.g., Jangid et al. [5], Makris et al. [6], Skinner et al. [11]). Of course, more sophisticated laws can be found in the scientific literature, requiring the identification of the parameters characterizing the behaviour of the isolators and dampers, but the simplified models shown above are generally preferred to carry out extensive numerical investigations.

The large base displacement due to strong near-fault ground motions can be enabled adopting large elastomeric bearings (e.g., increasing the dimensions of the rubber layers, for the HDLRB, and also the lead plug, for the LRB); analogous considerations apply to frictional bearings (e.g., gradually increasing the curvature and the roughness of the sliding surface, for the FP). In alternative, it is possible to combine elastomeric and steel-PTFE sliding bearings acting in series (e.g., as in the “Electricité-de-France” system, EDF), or HDLRBs placed on different layers and connected by steel plates (Skinner et al. [11], Morikawa et al. [12]).

A different approach is that based on the reduction of the base displacement taking advantage of the hardening response that a HDLRB exhibits for a strain amplitude greater than that commonly considered in the aseismic design, or through an in-parallel combination of a HDLRB and a supplemental damper. Actually a wide variety of energy dissipating devices is available, differing by the way of dissipating energy: friction, metallic-yielding, viscoelasticity and viscosity of elastomers or fluids (Soong et al. [13]). Moreover, particular devices are those based on electrorheological and magnetorheological fluids with a viscous-plastic behaviour (Makris [14]), or those made of nickel-titanium shape memory alloys (Dolce et al. [7]). At last, elastomeric and frictional bearings can be also combined in parallel (like in the “Resilient-Friction Base Isolator”, R-FBI). However, all these systems have the problem of increasing the contribution of the higher vibration modes of the superstructure.

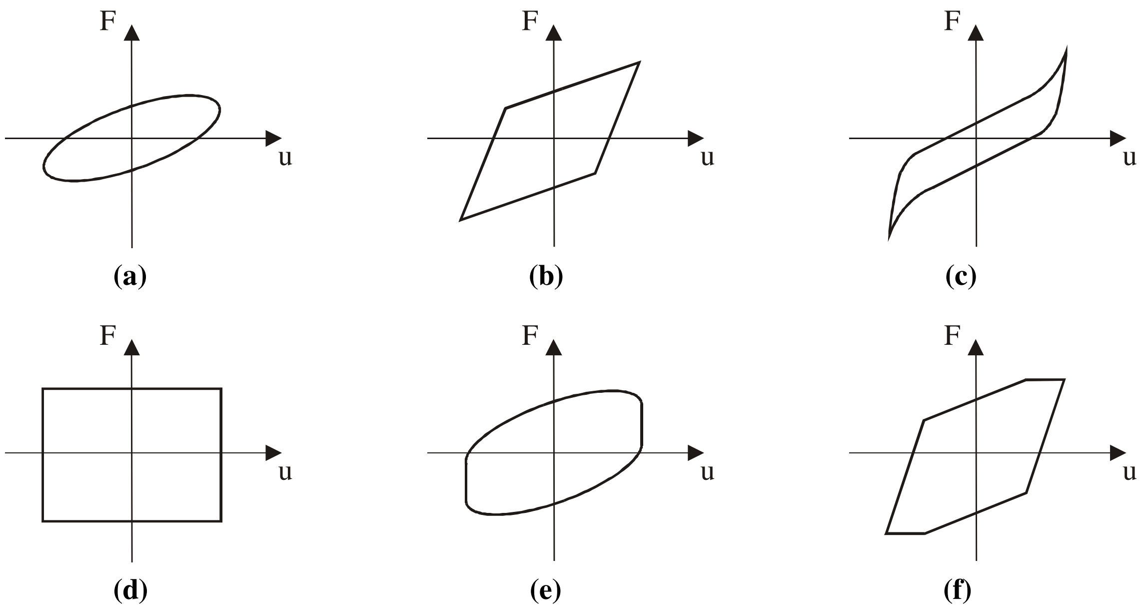

Figure 1: Response of base-isolation systems.

TEST STRUCTURES AND NEAR-FAULT GROUND MOTIONS

In the numerical investigation, whose results will be discussed in the following section, a base-isolated five-storey r.c. framed building is considered as reference test structure (figure 2a). Because of the structural symmetry and assuming the floor slabs be infinitely rigid in their own plane, the entire structure is idealized as an equivalent plane frame (figure 2b), whose elements have stiffness and strength properties so that the perimeter frames and the interior ones are represented as a whole (in the hypothesis that also the interior frames have the same characteristics). A grid of rigid girders is supposed placed at the base of the framed structure on the HDLRBs, assuming that an isolator corresponding to an interior column has a horizontal-section area twice as large as that of an isolator corresponding to an exterior column.

With reference to the same structural scheme (figure 2b), six cases of base-isolated structures, obtained considering three fundamental vibration periods (i.e., T_I=2s, 3s and 4s) and two subsoil conditions according to EC8 (i.e., subsoil classes A and D corresponding, respectively, to rock and moderately soft soil), are examined. For the sake of clearness, each base-isolated frame (BI) is labelled by using two characters after the BI acronym: the first one (2, 3 or 4) indicates the value of T_I in seconds, while the second one (A or D) the subsoil class. The design of the test structures is carried out with reference to the EC8 acceleration response spectra, considering: "full isolation" (i.e., the behaviour factor q is assumed equal to 1); high-risk seismic region with magnitude M_s>5.5 (peak ground acceleration: PGA=0.35g or 0.47g, for subsoil class A or D, respectively). The gravity loads used in the design are represented by dead- and live-loads, respectively equal to: 4.3 kN/m^2 and 1 kN/m^2, for the top floor; 5 kN/m^2 and 2 kN/m^2, for the other floors. The weight of the masonry infills, assumed as non-structural elements regularly distributed in elevation, is taken into account considering a vertical force of 3 kN/m^2. The effects of the seismic actions are evaluated according to EC8, assuming the masses associated with the dead-loads and the quasi-permanent values of the live-loads. At last, a mass equal to 1.5 times that of the first floor is considered at the base level. The cross-section dimensions of the girders and the columns are reported in table 1, with regard to the structures designed for rock (subsoil class A) and moderately soft soil (subsoil class D), while in table 2 are shown the equivalent stiffness (K_I) and the equivalent viscous damping (C_I) of the HDLRBs, which are evaluated according to the design displacement imposed by EC8.

A cylindrical compressive strength of 30 N/mm^2 for the concrete and a yield strength of 435 N/mm^2 for the steel are considered for the r.c. frame members. The design of the superstructure is carried out, in the six examined cases (three for each subsoil class), satisfying minimum conditions for the longitudinal bars of the girders and the columns: at least two 12 mm bars were provided both top and bottom throughout the length of all the members; for the girders, a tension reinforcement ratio not less than 0.15% is provided and, at their end sections, a compression reinforcement not less than half of the tension reinforcement is placed; for the symmetrically reinforced section of the columns, a minimum steel geometric ratio of 0.3% is assumed. Moreover, to prevent the formation of a soft-storey mechanism, the capacity design criterion of EC8 (i.e., that regarding the beam-column moment ratio, greater than or equal to 1.35, to have a "strong-columns weak-beams mechanism") is satisfied in all the beam-column joints, except at the top level where it is waived.

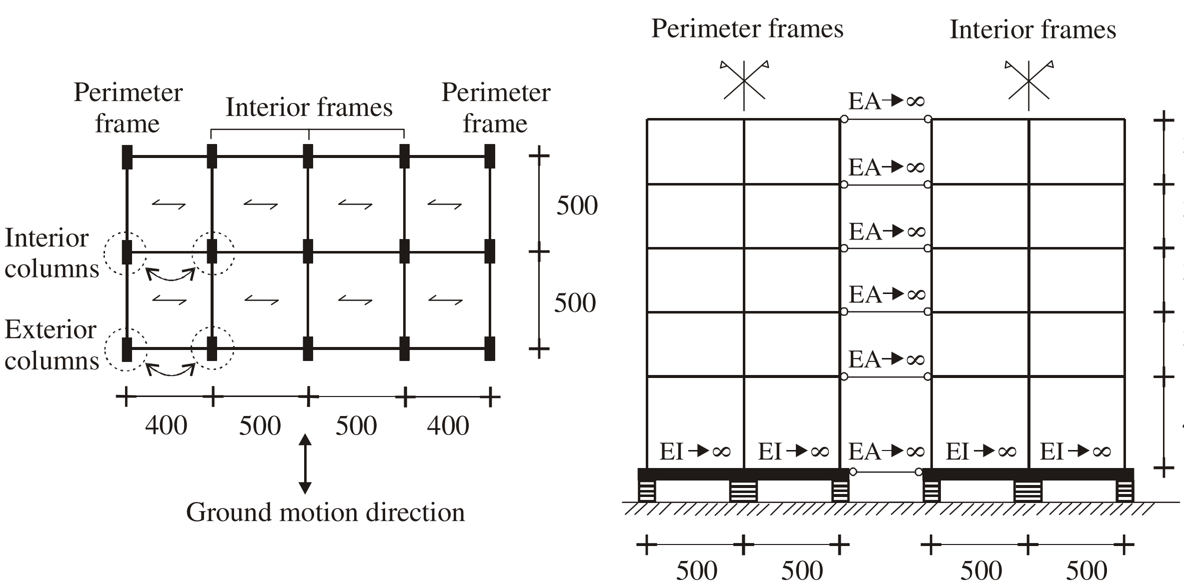

(a) Plan of the framed structure. **(b) Plane structure equivalent to that spatial.**

Figure 2: Base-isolated r.c. test structure (dimensions in cm).

Table 1: Section dimensions (in cm) of the r.c. frame members.

	Girders					
Storey	BI2.A	BI3.A	BI4.A	BI2.D	BI3.D	BI4.D
5	30x45	30x45	30x45	30x50	30x45	30x45
4	30x50	30x45	30x45	30x50	30x50	30x45
3	30x50	30x45	30x45	30x60	30x50	30x45
2	30x60	30x45	30x45	40x60	30x60	30x45
1	30x60	30x45	30x45	40x70	30x60	30x45
	Columns					
Storey	BI2.A	BI3.A	BI4.A	BI2.D	BI3.D	BI4.D
5	30x30	30x30	30x30	30x40	30x30	30x30
4	30x40	30x30	30x30	30x50	30x40	30x30
3	30x50	30x40	30x35	30x60	30x50	30x40
2	30x60	30x40	30x40	40x60	30x60	30x40
1	30x60	30x50	30x40	40x70	30x60	30x50

Table 2: Mechanical properties of the base-isolation systems.

	K_I (kN/cm)			C_I (kNs/cm)		
Isolators (HDLRBs)	BI2.A(D)	BI3.A(D)	BI4.A(D)	BI2.A(D)	BI3.A(D)	BI4.A(D)
Exterior	10.20	4.28	2.33	0.65	0.41	0.30
Interior	20.40	8.56	4.66	1.30	0.82	0.60

To study the seismic response of the test structures, near-fault accelerograms recorded in Turkey (1999, 2003) and in Greece (1986, 1999) are selected from the European Strong motion Database, which has been developed by the European Commission for Community Research [15]. In table 3 are indicated for the near-fault ground motions recorded in Turkey (which turned out to be the most severe for the examined structures): name of the recording station and its distances from the epicentre (Δ_e) and the fault (Δ_f), soil type, magnitude (M_w) and peak ground acceleration for the two horizontal components (PGA_{N-S} and PGA_{E-W}). In the figures 3a-3b and 4a-4b are compared, separately for the subsoil classes A and D, the curves representing the absolute input energy spectra for unit of mass (Uang et al. [16]) and the relative displacement spectra, obtained assuming an equivalent damping ratio ξ=12%. These curves are compared with those based on EC8 spectra for rock (EC8.A; PGA=0.35g) and moderately soft soil (EC8.D; PGA=0.47g); in particular, the input energy spectra are obtained assuming artificially generated accelerograms. As can be observed, EC8 spectral values are in many cases exceeded by those for near-fault ground motions, especially in the range of the rather long vibration periods (T≥2s), corresponding to the examined base-isolated structures; this behaviour is more evident for the curves corresponding to the Izmit-YP (Yarimca-Petkim) earthquake, which are plotted in the figures 4a-4b. Moreover, the Izmit-YP spectral values resulted generally greater than those for the Duzce earthquake (always for T≥2s), although both the horizontal components of this last one are characterized by PGA values higher than those of the Izmit Y-P earthquake.

Table 3: Near-fault ground motions recorded in Turkey.

Earthquake	Station	Δ_e (km)	Δ_f (km)	Soil	M_w	PGA_{N-S}	PGA_{E-W}
Izmit, 17/08/1999	Izmit	9	5	rock	7.6	0.16g	0.22g
Bingol, 01/05/2003	Bayindirlik	14	-	rock	6.3	0.52g	0.30g
Izmit, 17/08/1999	Yarimca-Petkim	20	5	soft	7.6	0.30g	0.24g
Duzce, 12/11/1999	Mudurlugu	8	0	soft	7.2	0.38g	0.51g

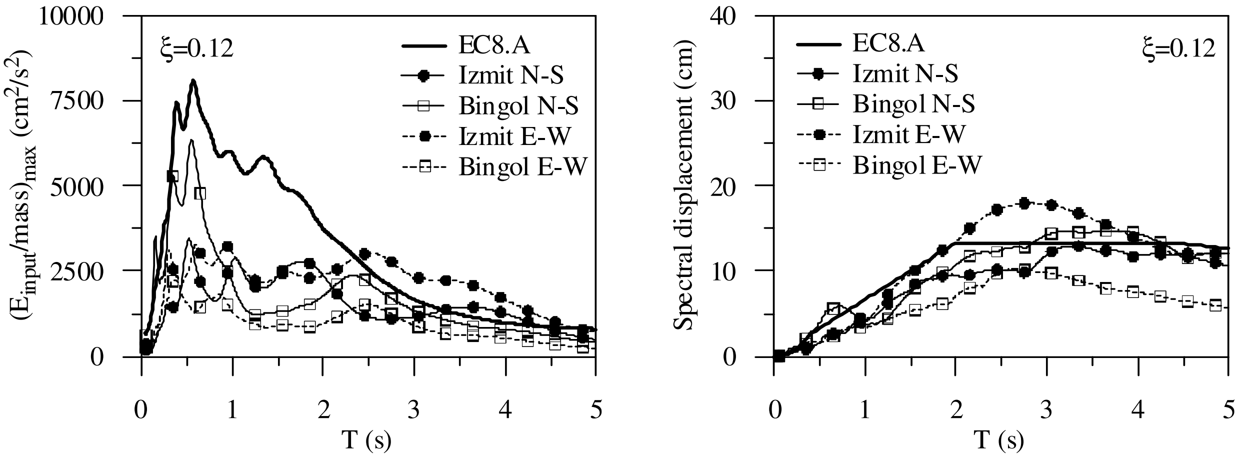

(a) **(b)**

Figure 3: Elastic response spectra (rock).

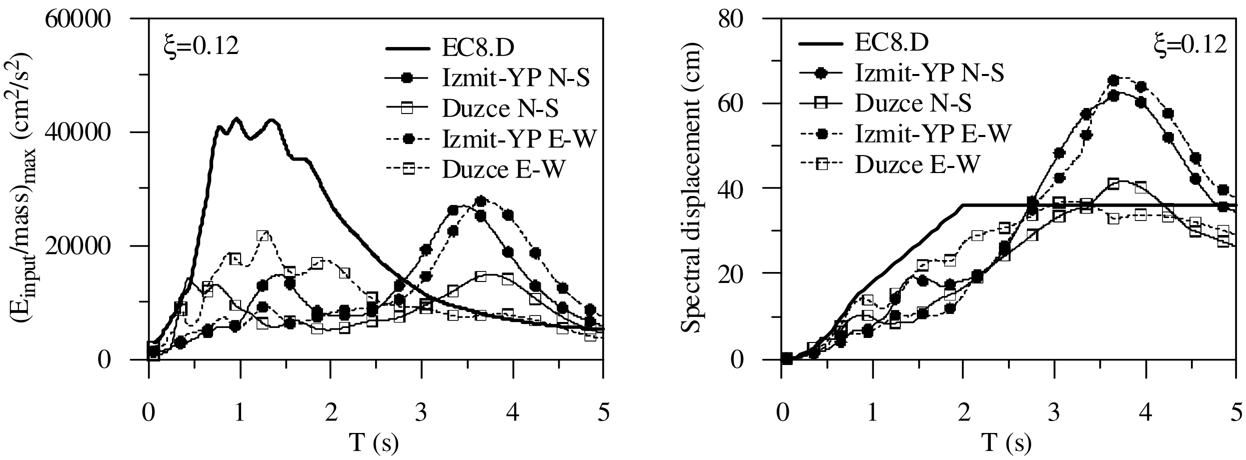

(a) **(b)**

Figure 4: Elastic response spectra (moderately soft soil).

NUMERICAL RESULTS

To study the effects produced by the insertion of supplemental viscous dampers or steel-PTFE sliding bearings, combined with the elastomeric bearings (HDLRBs), the isolated structure in figure 2b is considered as a reference. A numerical investigation is carried out to evaluate the nonlinear response of the structures subjected to strong near-fault ground motions, assuming that different combinations and arrangements of the supplemental devices (viscous dampers or sliding bearings) are adopted.

The nonlinear analysis is carried out using a step-by-step procedure based on a two-parameters implicit integration scheme and an initial-stress iterative procedure (Mazza et al. [3], Vestroni et al. [4]). At each step of the analysis, plastic conditions are checked at the end sections of the beams and columns, assuming a bilinear moment-curvature law with a hardening ratio of 2%. Moreover, axial strains are assumed fully elastic, while the shear deformation and the P-Δ effect are neglected; the effect of the axial load on the yield moment of the columns (M-N interaction) is also considered. The response of a HDLRB-type isolator is idealized assuming a very rigid truss element in the vertical direction and a horizontal truss element with an equivalent viscoelastic linear behaviour; a viscous-linear law and a rigid-plastic one are assumed to simulate the seismic behaviour of a supplemental damper and a sliding bearing, respectively.

The results obtained for the base-isolated systems are separately discussed below with reference to cases in which the HDLRBs are combined: (a) in parallel with supplemental viscous dampers (Base Isolation with in-Parallel Dissipation system: BIPD); (b) in parallel with steel-PTFE sliding bearings (Base Isolation with in-Parallel Sliding system: BIPS); (c) in series with steel-PTFE sliding bearings (Base Isolation with in-Series Sliding system: BISS). These results are compared with those obtained for the structures isolated only with HDLRBs (Base Isolation system: BI). For the sake of brevity, only results for the structures designed on moderately soft soil (BI2.D, BI3.D and BI4.D) will be presented, because the seismic response has been mainly elastic for those designed on rock (BI2.A, BI3.A and BI4.A).

Results for Base Isolation with in-Parallel Dissipation system (BIPD)

At first, the nonlinear response of the test structure shown in figure 2b, assumed with (in the BIPD system) or without (in the BI system) supplemental viscous dissipation at the base, is studied. The equivalent damping ratio of the supplemental base viscous dampers (ξ_D) is taken in the range 0.10÷0.50.

In figure 5 the maximum values attained at the isolators' top by the relative displacement are plotted against the equivalent damping ratio of the supplemental viscous dampers ξ_D (in particular, ξ_D=0 corresponds to a BI structure), under the two horizontal components of the Izmit-YP (figure 5a) and Duzce (figure 5b) earthquakes and for the three considered values of the fundamental vibration period of the BI structure (T_I=2s, 3s and 4s). In the figures 5a-5b a dashed thin line represents the spectral displacement imposed by EC8, which is constant in the range of vibration periods selected for the BI structures (see figure 4b). As can be observed, the isolators' displacement shows an increasing trend with T_I and attains the highest values practically in all the cases under the N-S component of the Izmit-YP earthquake (figure 5a) and the E-W component of the Duzce earthquake (figure 5b). The additional viscous damping at the base proves to be always favourable to control the isolator displacement, so avoiding too large isolators. More precisely, in all the examined cases the choice of increasing the ξ_D value produces the reduction of the isolator displacement, even though, for a same increase of ξ_D, this effect is ever-smaller. Moreover, it is worth to note that the insertion of the supplemental viscous dampers does not need re-centring of the isolation system at the end of the seismic input.

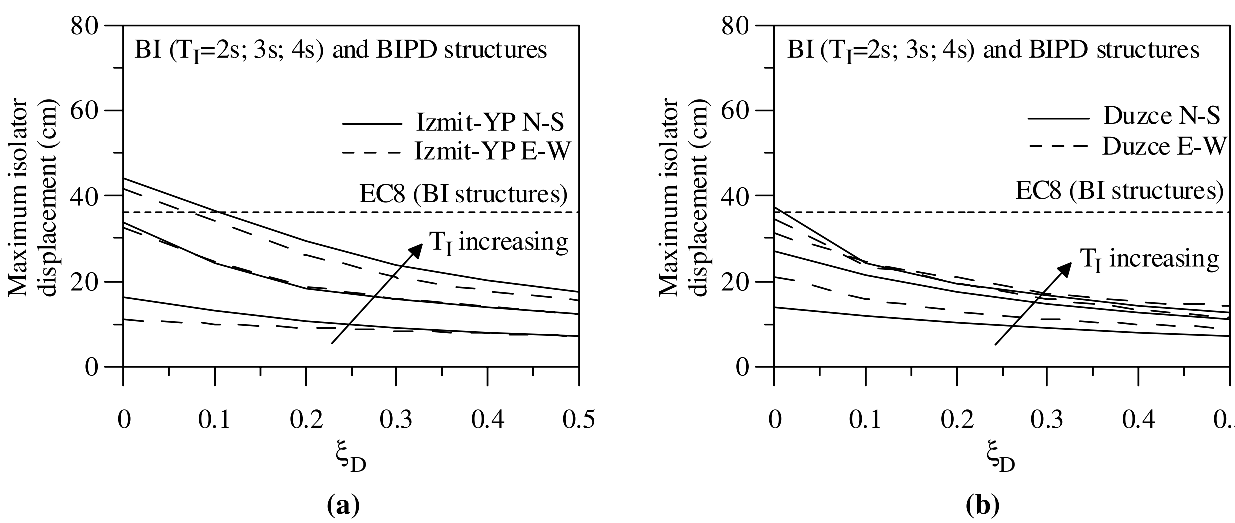

Figure 5: Maximum isolator displacement for increasing values of the supplemental viscous damping ratio ξ_D.

In figure 6 curves obtained for the base-isolated structure which underwent major damage of the r.c. frame members (BI4.D) are compared with the analogous curves when supplemental viscous dampers are added at the base (BIPD4.D). More precisely, the maximum values of the ductility demand for the girders are plotted along the frame height, assuming different values of ξ_D in the range 0.10÷0.50, under the N-S component of the Izmit-YP earthquake (figure 6a) and the E-W component of the Duzce earthquake (figure 6b). At least under the Izmit-YP earthquake, the ductility demand for the girders proves to be large enough without supplemental viscous damping (BI4.D structure), in spite of the nominal value assigned to the behaviour factor (q=1). Analogous results, which are omitted for the sake of brevity, have been obtained with reference to the columns, even though the "strong-columns weak-beams" mechanism led to low values of the ductility demand. Moreover, figure 6b underlines that the supplemental dissipation is not always favourable, depending on the characteristics of the seismic input. In particular, the curves obtained for the selected near-fault ground motions present an opposite trend in case a supplemental viscous dissipation is added at the base: an increasing value of ξ_D proves to be favourable under the N-S component of Izmit Y-P earthquake (figure 6a), while it is generally unfavourable, especially at the higher storeys, under the E-W component of Duzce earthquake (figure 6b). At last, the additional damping has been very effective under the N-S component of Izmit-YP earthquake, even assuming ξ_D=0.10, which is the lower value between those considered.

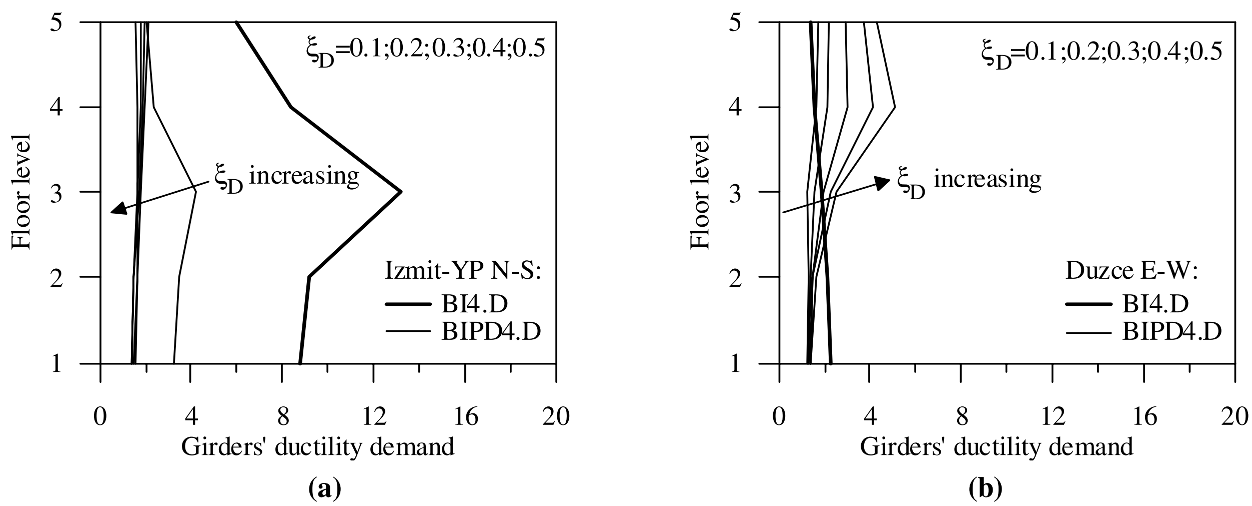

Figure 6: Girders' ductility demand for increasing values of the supplemental viscous damping ratio ξ_D.

Results for Base Isolation with in-Parallel Sliding system (BIPS)

In the second part of this study the response of the test structure shown in figure 2a (BI) has been compared with that of the structure obtained by the insertion of in-parallel sliding bearings (i.e., the BIPS system), under the Izmit-YP and Duzce earthquakes. In particular, it is assumed that the axial load in a column of the structure BIPS is split into equal contributions transmitted to the corresponding HDLRB and sliding bearing, when this last one is present. In figure 7 the arrangements of the elastomeric and sliding bearings considered in the present work are schematically shown. Each arrangement corresponds to a value of the sliding ratio $\alpha_S(=F_S/F_{S,max})$, defined as the global sliding force corresponding to the examined BIPS solution (F_S) divided by the maximum sliding force ($F_{S,max}$), this last one evaluated supposing that the elastomeric and sliding bearings are placed under each column. More precisely, the sliding force is evaluated assuming a friction coefficient μ=2% and considering, for the sake of simplicity, only the axial load in the columns evaluated under the gravity load combination. It is worth to mention that solutions different from those shown in figure 7 can be associated to a same value of α_S, choosing in a suitable way the arrangement of the elastomeric and/or sliding bearings.

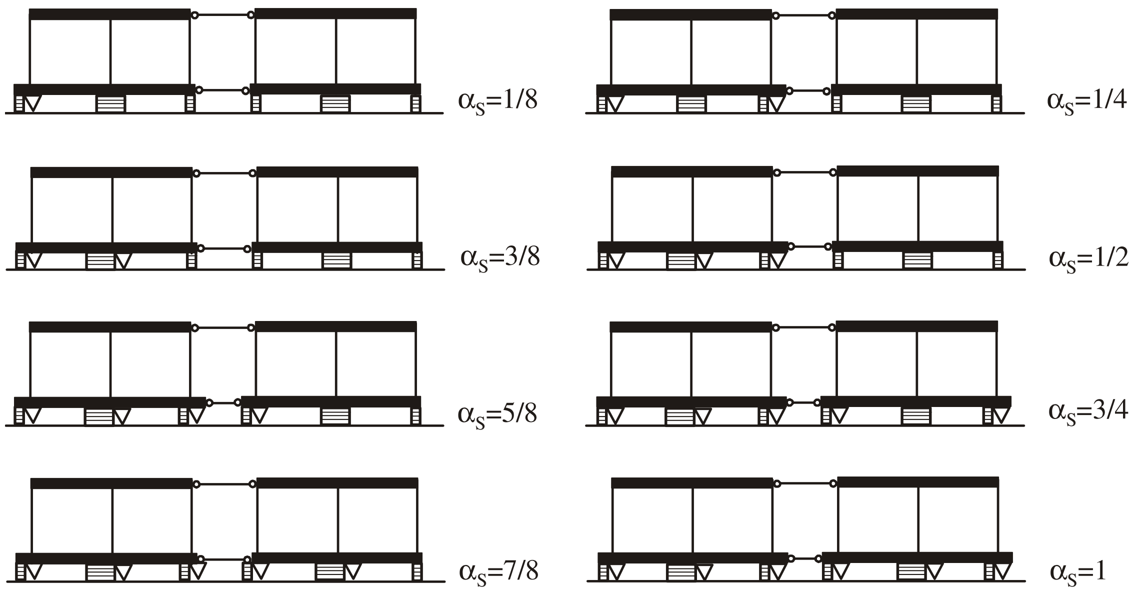

Figure 7: Arrangements of HDLRBs with in-Parallel Sliding systems (BIPS).

In figure 8 the maximum values attained at the isolators' top by the relative displacement, under each of the two horizontal components of the Izmit-YP earthquake (figure 8a) and the Duzce one (figure 8b), are plotted against the sliding ratio α_S varying in the range 0÷1 (in particular, α_S=0 corresponds to the BI solution, while α_S=1 corresponds to the BIPS solution in which the sliding bearings are placed under each column). As can be observed, the insertion of the sliding bearings has been always favourable to control the isolators' top displacement: the choice of increasing the α_S value produces the reduction of the isolator displacement, even though this effect, for a same increase of α_S, is ever-smaller.

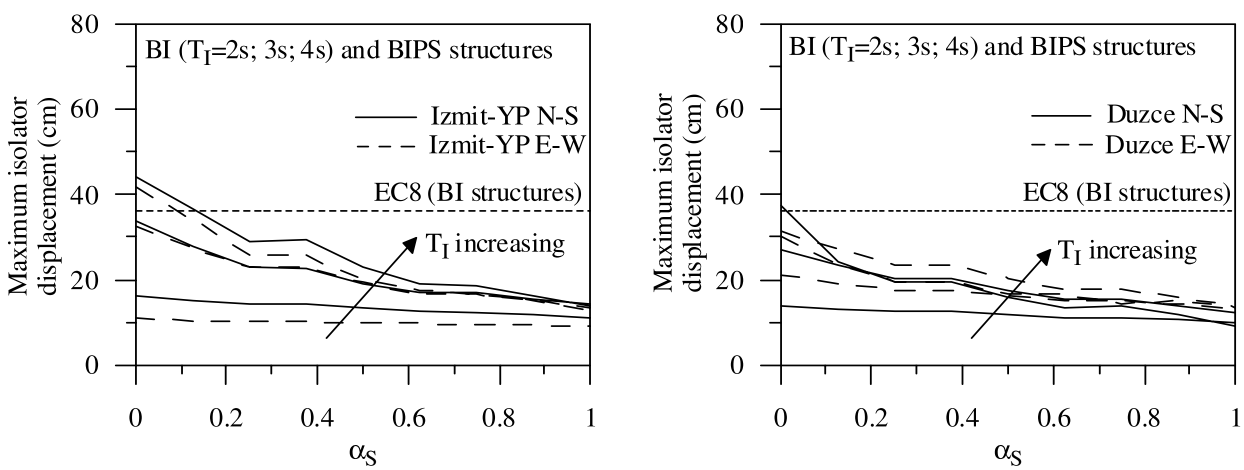

(a) **(b)**

Figure 8: Maximum isolator displacement for increasing values of the sliding ratio α_S.

It is worth to note that the re-centring of the isolation system may be needed when assuming rather high values of the sliding ratio α_S (i.e., in case further sliding bearings are added) and/or the friction coefficient μ. Indeed, at the end of the seismic input the percentage of the residual base displacement that can be recovered depends on the ratio between the restoring force produced by the HDLRBs and the overall friction threshold imposed by the sliding bearings. However, in all the examined cases the residual displacement of the base-isolation system, evaluated at an instant in which the post-earthquake vibrations practically stop, has been very little (figures 9a and 9b).

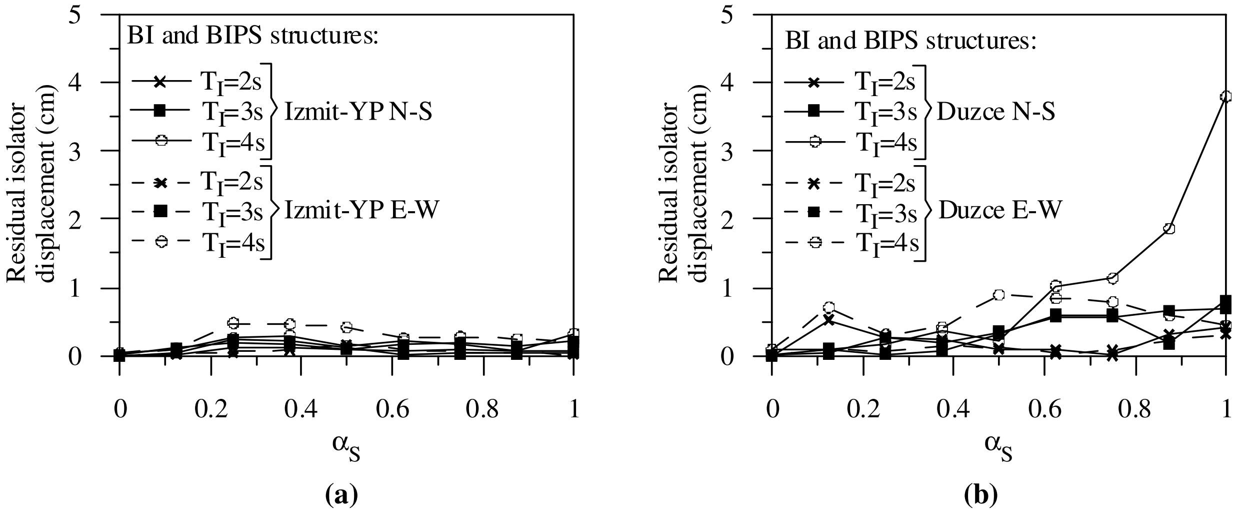

Figure 9: Residual isolator displacement for increasing values of the sliding ratio α_S.

To investigate about the effectiveness of the sliding bearings for controlling the local damage undergone by the critical end sections of the r.c. frame members, in figure 10 the mean values of the ductility demand for the girders are plotted along the frame height, with reference to the base-isolated structure BI4.D and to the corresponding structures with sliding bearings (BIPS4.D), assuming different values of α_S in the range 0÷1. More precisely, in the figures 10a and 10b are represented the curves obtained for a component of the Izmit-YP earthquake (N-S) and the Duzce one (E-W), respectively.

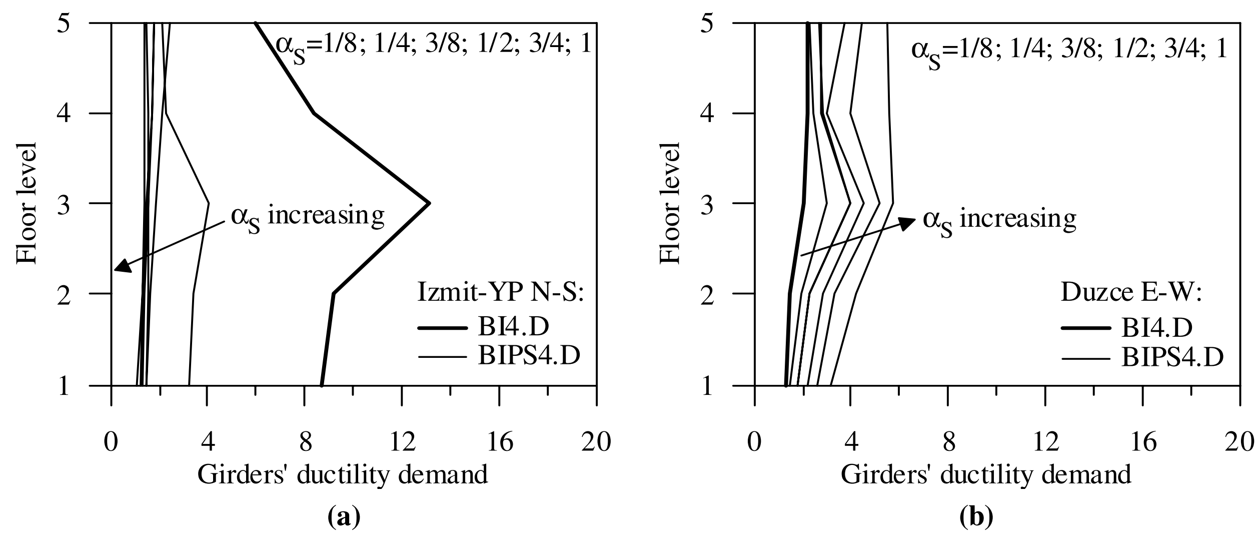

Figure 10: Girders' ductility demand for increasing values of the sliding ratio α_S.

The analysis of the results shows that the addition of sliding bearings acting in parallel with elastomeric isolators does not guarantee in all the cases a better performance of the superstructure. In particular, the performance under the E-W component of the Duzce motion (figure 10b) gets worse and worse for increasing values of α_S, because the structural behaviour becomes ever-closer to that of the fixed-base structure. On the other hand, the opposite trend is observed under the N-S component of the Izmit-YP motion (figure 10a), obtaining a basically elastic behaviour for increasing values of the sliding ratio (α_S>1/4). The different behaviour obtained for the two examined motions can be interpreted observing the corresponding energy spectra shown in figure 4a: the addition of sliding bearings (acting in parallel with the isolators) leads to a decrease of the fundamental vibration period, resulting favourable under the N-S component of the Izmit-YP motion and unfavourable, even though it is less evident, under the E-W component of the Duzce motion.

Results for Base Isolation with in-Series Sliding system (BISS)

At last, the response of the test structure shown in figure 2b (BI) has been compared with that of the structure obtained after the insertion of sliding bearings in series with the HDLRBs (i.e., the BISS system). In figure 11, the arrangements of the elastomeric and sliding bearings considered in the numerical analysis are schematically shown. The sliding ratio α_S, for each arrangement of the sliding bearings, has been assumed equal to that of the analogous BIPS system. However, it is worth to mention that a BISS solution presents a sliding force twice as large as that exhibited by the corresponding BIPS one, characterized by the same values of α_S and μ, because each sliding bearing is subjected to the whole axial load transmitted by the column when an in-series combination is adopted.

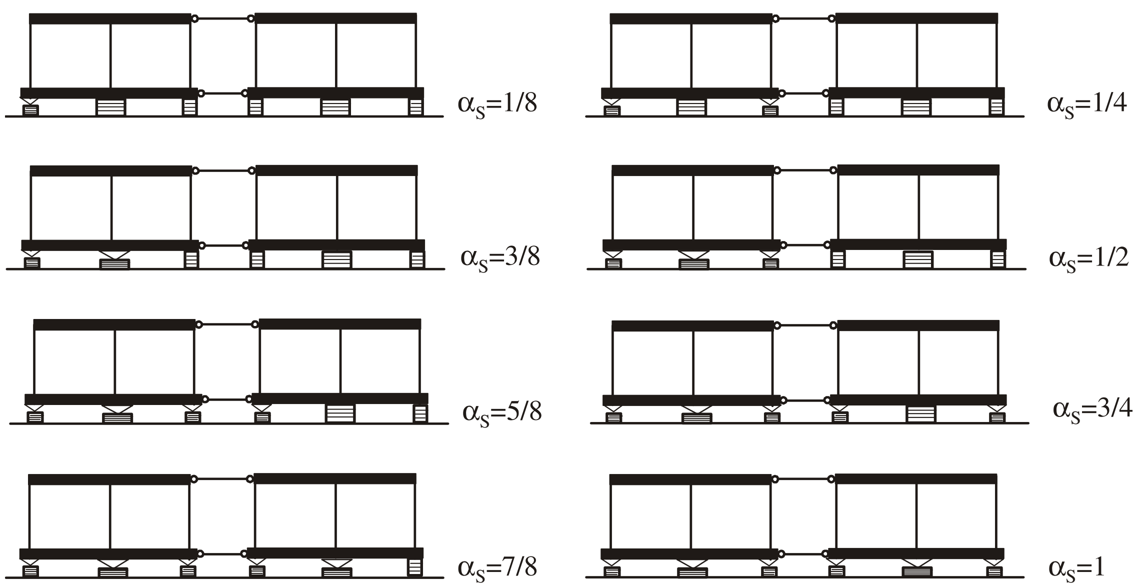

Figure 11: Arrangements of HDLRBs with in-Series Sliding systems (BISS).

Firstly, the effectiveness of the BISS system in order to control the displacement undergone by the base-isolation system has been investigated. To this aim, in the figures 12a-12b and 13a-13b are respectively plotted the maximum relative displacement of the elastomeric bearings and the residual base displacement of the superstructure, both against the sliding ratio α_S, varying in the range 0÷1. More precisely, the results have been obtained with reference to the horizontal components of the Izmit-YP (figures 12a and 13a) and Duzce (figures 12b and 13b) earthquakes. It is interesting to note that the maximum displacement is not equal for all the elastomeric bearings, unlike the base-isolation systems already examined (i.e., the BIPD and BIPS systems): as a proof of that, the isolators on which the sliding bearings are placed underwent displacements much less than the other ones, apart from the case corresponding to a sliding ratio α_S=1, in which all the isolators show comparable displacements. As can be observed from the curves plotted in the figures 12a and 12b, the addition of sliding bearings (i.e., the assumption of increasing values of α_S) does not correspond always to a reduction of the maximum relative displacement of the isolators. In particular, the spectral displacement imposed by EC8 is exceeded in many cases under the Izmit-YP earthquake (figure 12a), obtaining a considerable reduction of the maximum relative displacement only for the solution with sliding bearings placed on all the elastomeric isolators (i.e., for α_S=1). This kind of behaviour can be interpreted observing that the higher energy dissipation and the trend towards an amplification of the fundamental vibration period, as a consequence of the assumption of increasing values of α_S, are not always such as to balance the increased deformability of the base isolation system, when an in-series combination of the elastomeric and sliding bearings is adopted. On the other hand, the residual base displacement of the superstructure (figures 13a and 13b) proves to be, for both the examined earthquakes, practically negligible for $\alpha_S \leq 5/8$, while it reaches very high values for α_S=1. In this case, the re-centring of the isolation system after the earthquake may present, unlike the BIPS system, some difficulty, since out-of-phase movements between the isolators and the sliding bearings placed on them may take place.

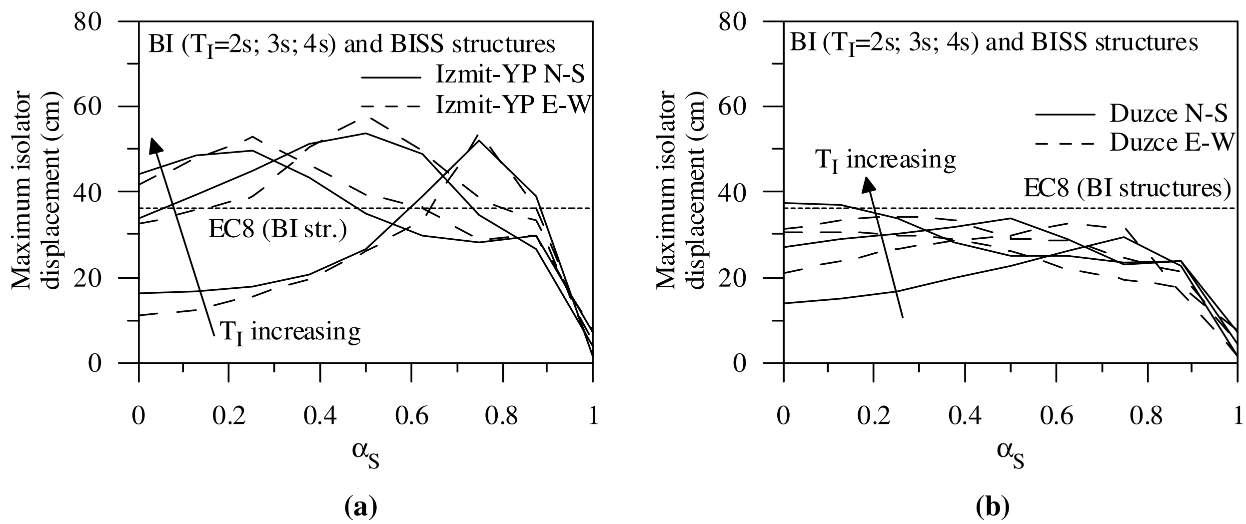

Figure 12: Maximum isolator displacement for increasing values of the sliding ratio α_S.

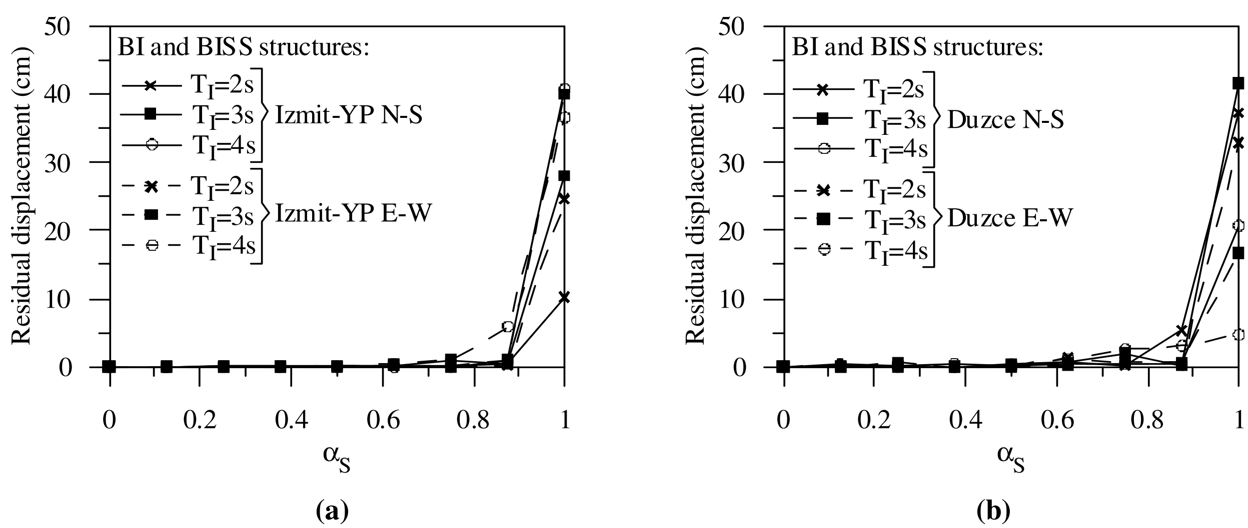

Figure 13: Residual base displacement of the superstructure for increasing values of the sliding ratio α_S.

Finally, in figure 14 are plotted curves representing, for the acceleration components considered in the analyses (i.e., N-S of Izmit-YP and E-W of Duzce motions), the ductility demand for the girders against the sliding ratio α_S. It is interesting to note that a considerable improvement of the structural performance is obtained for increasing values of α_S, especially under the N-S component of the Izmit-YP motion. Analogous results, which are omitted for the sake of brevity, have been obtained also with reference to the ductility demand for the columns and to the drift angle representing the non structural damage (e.g., that of infilled walls and partitions).

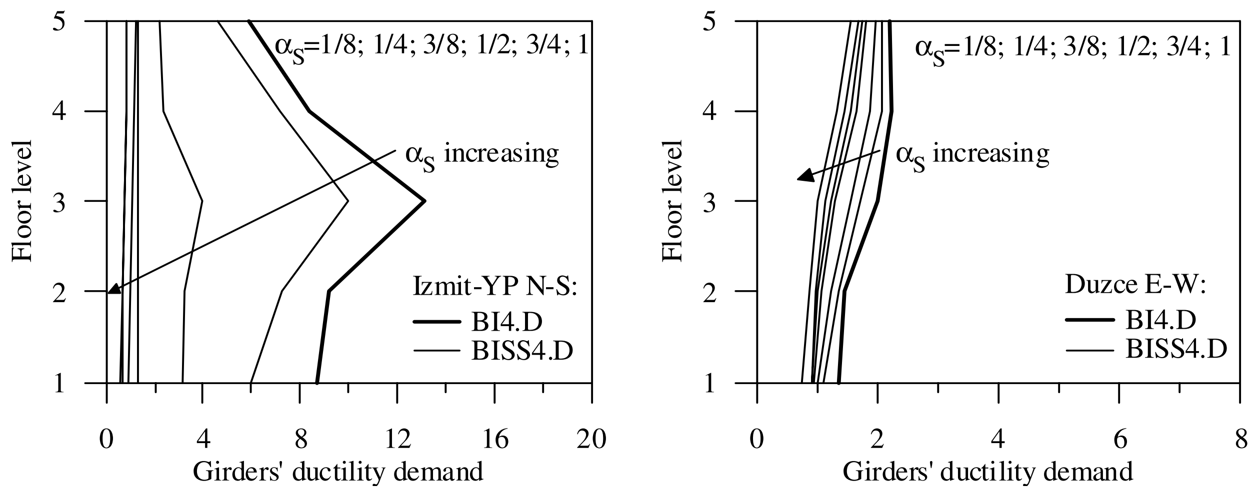

(a) **(b)**

Figure 14: Girders' ductility demand for increasing values of the sliding ratio α_S.

CONCLUSIONS

The nonlinear response of a typical five-storey r.c. framed building with different base-isolation systems has been studied under strong near-fault ground motions. In particular, a first solution with HDLRB-type isolators has been compared with different solutions obtained by means of the addition of viscous dampers (acting in parallel) or steel-PTFE sliding bearings (acting either in parallel or in series), assuming different values of the parameters characterizing the behaviour of the supplemental seismic devices. The following conclusions can be drawn from the results.

The in-parallel combination of isolators and viscous dampers (BIPD), as well as the analogous one with isolators and sliding bearings (BIPS), proved to be favourable for controlling the relative displacement of the isolators: the choice of increasing the equivalent damping ratio (ξ_D), for the BIPD system, or the sliding ratio (α_S), for the BIPS system, corresponds to a reduction of the isolator displacement, even though, for a same increase of ξ_D or α_S, this effect has been ever-smaller. However, the use of the BIPS system can need re-centring after an earthquake, in case the elastic restoring force produced by the elastomeric isolators does not exceed the friction threshold imposed by the sliding bearings. The in-series combination of isolators and sliding bearings (BISS) is not always favourable, for increasing values of α_S, in reducing the residual displacement of the isolation system. Moreover, the re-centring of this system may present some difficulty when the residual displacement is a combination of out-of-phase movements between the isolators and the sliding bearings placed on them.

With reference to the ductility demand for the r.c frame members, the adoption of the BIPD system or the

BIPS one does not guarantee in all the cases a better performance for increasing values of ξ_D or α_S, respectively. However, the BISS system proves to be generally effective for controlling the structural and non-structural damages of the framed building, producing an amplification of the fundamental vibration period and limiting the maximum acceleration transmitted to the superstructure.

The present work was partially financed by M.I.U.R.
(Italian Ministry of the Education, University and Research).

REFERENCES

1. Eurocode 8. "European Standard, Design of structures for earthquake resistance. Part 1: General rules, seismic actions and rules for buildings." Draft no. 6, 2003.
2. Kelly JM. "The role of damping in seismic isolation." Earthquake Engineering and Structural Dynamics 1999; 28: 1717-1720.
3. Mazza F, Vulcano A. "Seismic response of buildings with isolation & supplemental dissipation at the base." Proceedings of the 5th World Congress on Joints, Bearings and Seismic Systems for Concrete Structures, Rome, Italy, 2001, CD-ROM.
4. Vestroni F, Vulcano A, Di Pasquale G. "Earthquake response analysis of a nonlinear model of a base-isolated structure." Proceedings of the International Meeting on Earthquake Protection of Buildings, Ancona, Italy, 1991; 181/C-190/C.
5. Jangid RS, Kelly JM. "Base isolation for near-fault motions." Earthquake Engineering and Structural Dynamics 2001; 30: 691-707.
6. Makris N, Chang S-P. "Effect of viscous, viscoplastic and friction damping on the response of seismic isolated structures." Earthquake Engineering and Structural Dynamics 2000; 29: 85-107.
7. Dolce M, Cardone D, Nigro D, Ponzo FC, Nicoletti M, La Monaca B. "Experimental comparison between conventional and innovative base isolation systems on a 1:2:5 scaled reinforced concrete frame." Proceedings of the 12th European Conference on Earthquake Engineering, London, UK. Paper no. 746. Elsevier Science Ltd, 2002.
8. Naeim F, Kelly JM. "Design of seismic isolated structures." John Wiley and Sons, New York, USA, 1999.
9. Skinner RI, Robinson WH, McVerry GH. "An introduction to seismic isolation." John Wiley and Sons, Chichester, England, 1993.
10. Kelly JM. "Progress of application and R&D for seismic isolation for civil structures in the United States." Proceedings of the 7th International Seminar on Seismic Isolation, Passive Energy Dissipation and Active Control of Vibrations of Structures, Assisi, Italy, 2001. Paper no. L15.
11. Skinner RI, McVerry GH. "Seismic isolators for ground motions with large displacements and velocities." Proceedings of the 11th World Conference on Earthquake Engineering, Acapulco, Mexico, Paper no. 1841. Oxford: Pergamon, 1996.
12. Morikawa S, Masaki N, Suzuki S, Suizu Y. "Multi-Stage Rubber Bearings for Seismic Isolation." Proceedings of the International Meeting on Earthquake Protection of Buildings, Ancona, Italy, 125/C-134/C, 1991.
13. Soong TT, Dargush F. "Passive energy dissipation systems in structural engineering." John Wiley and Sons Ltd, England, 1997.
14. Makris N. "Rigidity-plasticity-viscosity: can electrorheological dampers protect base isolated structures from near-source ground motions?" Earthquake Engineering and Structural Dynamics 1997; 26: 571-591.
15. European Commission for Community Research. "European Strong motion Database (on-line)." www.isesd.cv.ic.ac.uk/ESD.
16. Uang C-M, Bertero VV. "Evaluation of seismic energy in structures." Earthquake Engineering and Structural Dynamics 1990; 19: 77-90.